Pharmaceutical Sciences, 2020, 26(Suppl 1), S52-S62
doi:10.34172/PS.2020.44
https://ps.tbzmed.ac.ir/

Research Article

In Silico Drug Repurposing of Penicillins to Target Main Protease M^{pro} of SARS-CoV-2

Krishnaprasad Baby[1], Swastika Maity[1], Chetan Mehta[2], Akhil Suresh[2], Usha Y Nayak[2], Yogendra Nayak[1*]

[1]*Department of Pharmacology, Manipal College of Pharmaceutical Sciences, Manipal Academy of Higher Education, Manipal. India – 576104.*

[2]*Department of Pharmaceutics, Manipal College of Pharmaceutical Sciences, Manipal Academy of Higher Education, Manipal. India – 576104.*

Article Info

Article History:
Received: 3 May 2020
Accepted: 29 May 2020
ePublished: 30 November 2020

Keywords:
-Beta-lactams
-COVID-19
-SARS-CoV-2
-M^{pro}
-Viral protease
-Virtual screening

Abstract

Background: SARS coronavirus-2 (SARS-CoV-2) infection causes Novel Coronavirus Disease (COVID-19). It is a respiratory tract infection and currently becoming pandemic worldwide affecting more than 50 lakh people. As of now, there is no treatment or vaccine developed for disease management. The main protease, M^{pro} in SARS-CoV-2 is a druggable target explored by many scientists. We targeted this with the well-known approach of drug repurposing by using computational tools.

Methods: Schrödinger software was used for the study. Ligands were prepared from US-FDA drug-bank by importing it to Maestro graphical user interphase, optimised using LigPrep, and molecular geometry minimized using OPLS3e force-field. M^{pro} crystal structure 6LU7 was downloaded from PDB and optimised. Molecules were docked using CovDock module in Glide docking. Further, molecular dynamics simulations were carried out for 100 ns using Desmond module.

Results: In docking and molecular interactions studies, penicillins emerged as hits with consistent binding pattern by forming hydrophilic, hydrophobic, electrostatic interactions. The molecular dynamics simulations confirmed the interactions. Phenoxymethylpenicillin and Carbenicillin were found to interact consistently and appeared to be the most promising.

Conclusion: Usually, antibiotics are discouraged from using in the viral pandemic because of the development of resistance. Azithromycin was combined with hydroxychloroquine to treat COVID-19. Penicillins are less potent and first-line antibiotics for most of the bacterial infections. This study suggests Phenoxymethylpenicillin and Carbenicillin can be tried along with hydroxychloroquine. Further, this study shows the possible exploration by drug repurposing using computer-aided docking tools and the potential roles of beta-lactams in COVID-19.

Introduction

Coronaviruses (CoVs) are the causative organism for severe infections in both humans and animals, which can cause disorder in the respiratory tract and digestive tract. Previous studies have reported that CoVs can infect organisms, including mammals such as bats, civets, camels and pangolins, avian species, and reptiles.[1-3] On December 27, 2019, Chinese patients were identified with extreme pneumonia at a hospital in Wuhan. The airway epithelial cells from bronchoalveolar-lavage fluid were detected with a novel virus of 60 to 140 nm diameter and 9 to 12 nm long spikes, resembled solar corona. Thus, the causative agents were identified as a novel coronavirus (n-CoV).[4] Initially, the virus was called as the 2019-novel coronavirus (2019-nCoV). On 12 January 2020, WHO called the disease as coronavirus disease 2019 (COVID-19). At the same time, International Committee on Taxonomy of Viruses (ICTV) named n-CoV as SARS-CoV-2.[5] CoV, generally spherical with spikes and have positive-sense single-stranded RNA (+ssRNA) of size 30 kb with RNA transcript 5'-cap and 3' poly-A tail. The genetic material in CoVs is highly susceptible to mutations, and there were incidences of altered virulence and human pandemic outbreaks. There are know mutants of CoVs which are causing diseases in humans are 229E, NL63, OC43, HKU1, the Middle East respiratory syndrome (MERS)-CoV, SARS)-CoV and the recent one SARS-CoV-2.[6] Further, the structure of CoV also has two groups of proteins characterized as structural and nonstructural proteins (NSPs). The structural proteins are membrane (M), envelope (E), spike (S), nucleocapsid (N) proteins. More than 50% of viral +ssRNA-genome is covered by the six open reading frames (ORFs) 1a/b, which produces the two viral replicases that are polyproteins 1a and 1ab (PP1a and PP1ab). The processing of these PPs by proteases encoded by ORF1a gives rise to sixteen mature nonstructural proteins (NSPs 1 to 16), which are currently known.[7]

*Corresponding Author: Yogendra Nayak, E-mail: yogendra.nayak@manipal.edu; yogendranayak@gmail.com

SARS-CoV-2 transmitted between people primarily through respiratory droplets or droplet nuclei and contact routes.[8,9] Transmission may also occur through fomites in the immediate environment around the infected person.[10] The presence of SARS-CoV-2 in faecal content suggests that COVID-19 might infect the population by the orofecal route. However, there are no accurate reports of orofecal transmission of the COVID-19 virus to date.[11] Once the droplet enters the body, usually through the nasal route, the spike proteins bind to the host cell receptor, and the viral-genome along with the nucleocapsid proteins enter the host cytoplasm. The host cell receptors for SARS-CoV-2 in COVID-19 is angiotensin-converting enzyme-2 (ACE-2).[12] Thus, targeting ACE-2 or the spike protein is an excellent strategy to prevent the virus entry inside the organism as well as for vaccine development.[13] Inside the host cells, the viral +ssRNA using RNA-dependent RNA-polymerase (RdRP; also called as NSP12) and replicates viral genomic RNA and subgenomic RNAs (sgRNAs).[14] The +ssRNA also uses the host ribosome and produces PPs by the process of transcription. The PPs are then converted into NSPs by the proteolytic process of specific proteases as encoded by ORFs in +ssRNA.[7] Among the frameshift ORF1a and ORF1b guide the production of both pp1a and pp1ab that are processed by virally encoded 33.8-kDa chymotrypsin-like protease ($3CL^{pro}$) or main protease (M^{pro}), as well as one or two papain-like proteases. The M^{pro} digests the polyprotein at not less than 11 conserved sites, starting with the autolytic cleavage of this enzyme itself from pp1a and pp1ab. Thus, M^{pro} is identified as a druggable target for anti-COVID-19 agents.[15–17] ORF1a and 1b produce 16 non-structural proteins (NSPs). Apart from ORF1a and ORF1b, other ORFs encode for structural proteins such as S, M, E, and N proteins. Further, the major part of NSPs such as S, M and E forms the replicase-transcriptase complex (RTC) and incorporated into a double-membrane vesicle. A copy of genomic +ssRNA with nucleocapsids (N) fuses with the vesicle and matures at the endoplasmic reticulum (ER)-Golgi intermediate compartment (ERGIC) complex. The freshly formed virus particles then bud out from the host cells by exocytosis process. Thus, the virions in the extracellular fluid will then enter another cell, and the cycle continues.[18]

In the lungs alveoli, the host cells are usually type-II alveolar cells or type-II pneumocytes which produce surfactants. When the cytosol is producing the viral proteins, the pneumocytes release inflammatory mediators. These inflammatory mediators then stimulate the alveolar macrophages to release proinflammatory cytokines such as interleukins (IL-1 and 6), and tumour necrotic factor α (TNF-α).[19] These cytokines enter into the bloodstream, leading to vasodilation and increase vascular permeability causes fluid accumulation, alveolar oedema and collapse. The alveolar collapse is the reason for decreased gas exchange and hypoxemia. It attracts more and more neutrophils leading to further release of proteins and reactive oxygen species (ROS) and total damage of alveoli. The damaging of massive alveoli leads to wheezing, dyspnea and cough. The proinflammatory cytokines also stimulate the production of specific prostaglandin in the hypothalamus. The prostaglandins then stimulate the thermoreceptor and increase body temperature. Hypoxemia stimulates the chemoreceptors, whereby increases the heart rate and breathing. Decreased oxygen and increased inflammation lead to increased chances of kidney and liver failure in susceptible patients. The surge of cytokines leads to septic shock, and ultimately the circulatory collapse causes the death.[20-22]

The drugs, chloroquine and hydroxychloroquine have mild antiviral activity but strong anti-inflammatory and immunomodulatory activity. They prevent the cytokine surge in COVID-19. On 19 March 2020, US-FDA approved limited emergency use for chloroquine and hydroxychloroquine for the treatment for COVID-19, though the clinical trials are underway.[23] Chloroquine supported viral infection, reduced pneumonia exacerbation, improved radiological findings and virus-negative conversion and shortened the course of the disease.[24] In combination with azithromycin, hydroxychloroquine exhibited higher rates of viral load reduction/disappearance.[25] Many possible drug candidates have been suggested as a therapy against COVID-19. They include lopinavir/ritonavir, nucleoside analogues, neuraminidase inhibitors, remdesivir, umifenovir, DNA synthesis inhibitors, and some conventional Chinese medicines.[26-29] Additionally, ACE2-based peptide, 3CLpro inhibitor (3CLpro-1) and a new vinyl sulfone protease blocker also appear to have a potential for antiviral action against SARS-CoV-2.[30] A randomized, controlled, open-label trial, conducted in adult patients with confirmed SARS-CoV-2 infection was conducted using lopinavir 400 mg and ritonavir 100 mg combination treatment. The result of this trial was not associated with any difference from standard care, but increased risk of gastrointestinal adverse events.[31] Similarly, the National Medical Products Administration of China approved the use of favipiravir, for the treatment for COVID-19. Favipiravir was approved for further clinical studies based on the success study with minimal side effects conducted in Shenzhen, Guangdong province of China in 70 patients.[32,33] The efficiency of molecules so proposed are in clinical trials for their beneficial effect against COVID-19. Vaccine development will take more than a year. Hence, drugs discovery scientists and the government agencies are shifting their focus on the repurposing of already known therapeutically used drugs, whereby the drug development would be faster than expected.

Recently, Zhenming Jin and group have identified potent irreversible inhibitor of M^{pro}. They explored computer-aided drug design (CADD) and emerged with six compounds potent inhibitor of M^{pro}. The compound N3 was highly potent among the six.[34] These molecules are now in the clinical trials. The literature is available now on M^{pro} simulations[15,17,35] These findings encouraged us to use

the computation tool for the repurposing of drugs as M^{pro} inhibitors. In this study, we have reported the molecular dynamics study of FDA approved β-lactams.

Materials and Methods

Computational simulations

All the computational simulations were carried out using Maestro graphical user interphase of Schrödinger (www.schrodinger.com) on a desktop workstation with Ubuntu platform, with Intel® Xenon® Gold 6130 CPU @ 2.10 GHz x 64 processors, Quadro P620/PCle/SSE2 graphics card and 134.8 GB ram.

Ligand preparation

The US-FDA approved molecules (n=2800) were downloaded from www.drugbank.ca. The molecules were optimized using LigPrep[36], wherein the 3D coordinates were generated for the molecules, Epik module predicted the correct ionization state at pH 7.4, the tautomer forms were generated, and proper chirality was defined. Finally, molecules were geometry minimized using OPLS3e force-field.[37]

Protein preparation

The protein structure of M^{pro} coordinate with accession code 6LU7 was downloaded from PDB (Protein Data Dank, www.rcsb.com). The Protein Prep Wizard (PPW) was used for the optimization of the protein structure.[38] The missing hydrogens, side chains, and residues were added, waters were deleted. Then using PROPKA the correct ionization state was generated at pH 7.4, and the hydrogen bond network was regenerated, and finally, protein structure was minimized.[39,40]

Docking

The Glide module was used for docking.[41] The binding site was specified on to a grid by considering the centroid of the bound ligand using Glide grid generation with the default option. The docking was run with SP (Standard Precision) method, and the single best pose was saved for each molecule.[42] Initially, 2800 US-FDA molecules were screened through SP. The β-lactams exhibited a good and consistent interaction by SP docking, and they were further studied by covalent docking.

The covalent docking was carried out using CovDock module[43] in Glide docking.[44] The Cys145 was specified as reactive residue to form the covalent reaction, and the β-lactam addition type of reaction was specified as a covalent reaction type with all other default parameters. The single best pose was saved for each molecule.

Molecular dynamics simulation

The MD simulation was run on Desmond module.[45] Using the System Builder tool in Desmond, the water-soaked solvated system was generated. The TIP3P model of water considered for solvating the system. The orthorhombic simulation was the box with periodic boundary condition generated with a buffer distance of minimum 10 Å from the outer surface of the protein. The system was neutralized by adding a suitable number of counter-ions. The isosmotic condition was maintained by adding 0.15 M NaCl to the simulation box. A predefined equilibration protocol was run before the production run of the simulation. The MD simulation was run at 300° K temperature at atmospheric pressure of 1.013 bar. A total of 100 nsec simulation was run during which 1000 frames were saved to the trajectory. The Simulation Interaction Diagram was used for the analysis of the MD simulation trajectory.

Results and discussion

M^{pro} protein target

In protein databank (PDB), the 6LU7 was the first crystal structure of M^{pro} from COVID-2.[34] The M^{pro} is reported drug-target both in SARS and MERS.[24] Protein M^{pro} is essential for viral replication.[46] There have been many research article where the researcher has reported inhibitors of this protein for SARS-CoV and MERS-CoV.[47] The importance of this protein in the viral replication cycle and absence of any close homologues protein in human counterpart makes M^{pro}, a very attractive target for the COVID-2 antiviral drug design. The 6LU7 is crystallized with N3, a Michael acceptor, which is reported to bind to M^{pro} of SARS-CoV and MERS-CoV. It covalently binds to the COVID-2 with amino acid residue Cys145 and exhibited a CC50 of around 133 µM. The N3 also exhibited to reduce the viral load in a cell line with the EC_{50} of 16.77 µM.[34] Based on these observations, we considered the M^{pro} to be an attractive target, and with the intentions of identifying the inhibitors of M^{pro}, we ran computational virtual screening.

Beta-lactam as hits and their binding mode

The FDA approved molecules was considered for virtual screening. The virtual screening was run to identify the non-covalent (reversible) binding mode. The docking results for few of the penicillin exhibited interesting binding mode. Ampicillin, benzylpenicillin and azidocillin not only exhibited complementing combination on polar non-polar interactions with M^{pro}, but the β-lactam ring also occupied space close to the residue Cys145. Figure 1 shows the binding mode of ampicillin, benzylpenicillin and azidocillin predicted by docking (non-covalent). The amine group in these penicillins formed H-bond interaction with residue His164, the carbonyl group in amide and carbonyl group of the β-lactam ring formed bifurcated H-bond with residue Cys145, the carboxylate group formed H-bond with residue Thr26; the phenyl group formed the π-π staking interaction with His41; the residues His41, Met49, Cys145, Met165 etc., formed hydrophobic interactions. The benzylpenicillin addition to above-mentioned interactions it exhibited H- bond with Gly43, and the azidocillin exhibited H-bond with Gly43 and additional H-bond between the azide group and Glu166. The distance between the Cys145 thiolate group and β-lactam ring in ampicillin, benzylpenicillin and azidocillin were found

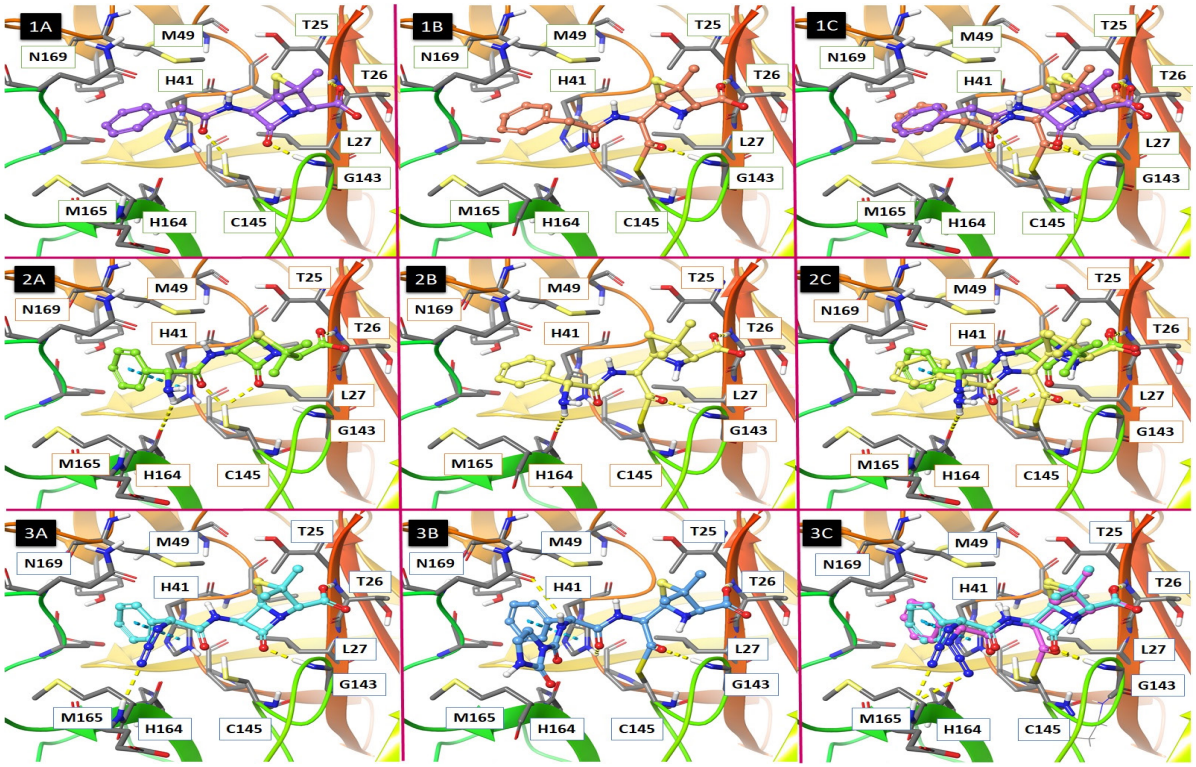

Figure 1. Binding mode comparison 1: Ampicillin; 2: Benzylepenicillin; 3: Azidocillin; A: Reversible docking; B: Covalent docking; C: Superimposed pose of reversible and covalent docking with M^{pro}.

2.37 Å, 3.26 Å and 3.21 Å respectively.

Covalent docking

The penicillin with the β-lactam ring has been reported earlier as antiviral protease inhibitors[48,49], but they were not explored further as better antiviral agents were existing. Also, like N3 inhibitor, there were several molecules reported being covalent inhibitors of M^{pro} for SARS-CoV and MERS-CoV.[34] This leads us to think about the possibility of formation of covalent binding of penicillin with M^{pro} protein through amino acid residue Cys145. The CovDock protocol in Schrödinger follows three steps. In the first step, the covalent reactive residue is mutated to Alanine. To this modified receptor, the ligand will be docked and the all the poses where the reactive moiety form the ligand falls close within 3.5 Å distance will be considered for the next step where the covalent bond will be built, and the complex will be minimized. The β-lactam ring occupied the space close to the thiol group of cysteine in the SP docked poses of the penicillin. In reality, to form a covalent bond the reactive residue of protein and the reactive group in the ligand should come close so that they can for the chemical reaction resulting in the formation of a chemical bond. To check this, ampicillin, benzylpenicillin and azidocillin were subjected to the covalent docking using CovDock protocol, with 'β-lactam ring addition' type of reaction and the Cys145 was as the red as the reactive residue. The covalent docked pose for ampicillin, benzylpenicillin and azidocillin with M^{pro} is shown in Figure 2.

The covalent bound pose of the azidocillin, benzylpenicillin

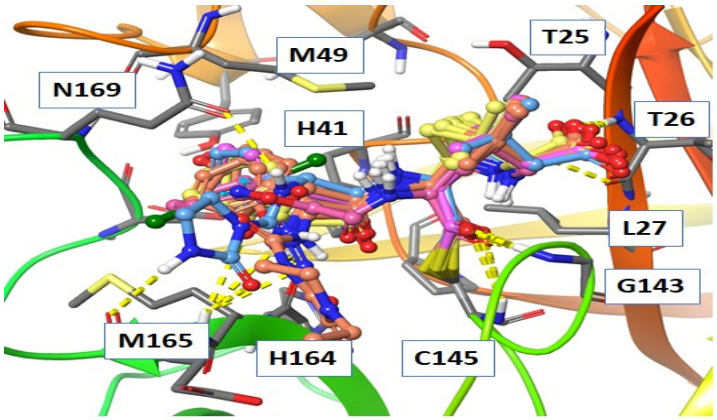

Figure 2. Superimposed covalent docking pose depicting the consistent binding mode for Amoxicillin, Ampicillin, Azidocillin, Azlocillin, Benzylpenicillin, Carbenicillin, Dicloxacillin, Phenoxymethylpenicillin and Piperacillin. The yellow colour dotted line represents the H-bond, cyan colour dotted line represents the π-π staking interaction

and azidocillin exhibited same binding mode and interaction pattern and contact residues as that observed in the non-covalent binding mode. The RMSD (root mean square deviation) between the covalent and non-covalent docked pose for Ampicillin was 1.10 Å; for Benzylpenicillin it was 0.92 Å, and for Azidocillin it was found to be 0.78 Å. The RMSD within 2 Å indicated that even after covalent bond formation same binding mode was retained by all the ligands. Figure 2 is the snapshot of superimposed covalent, and non-covalent docked pose of selected penicillins.

There are 36 molecules with β-lactam rings which are FDA approved including penicillins and cephalosporins. All these molecules were subjected to the covalent docking. Examination of the resulting covalent bond poses exhibited a consistent binding mode for about nine of the penicillins. Amoxicillin, ampicillin, azidocillin, azlocillin, benzylpenicillin, carbenicillin, dicloxacillin, phenoxymethylpenicillin and piperacillin exhibited same binding orientation and interaction pattern and contact residues. Figure 2 shows the superimposed covalent binding mode of all these penicillins. Table 1 lists all the polar and nonpolar interactions observed between these penicillins and the M^{pro} protein.

Binding Interactions of Covalent Docked Beta-lactam Molecules

The covalent docked pose of the amoxicillin exhibited a blend of polar and non-polar interactions with M^{pro} protein

Table 1. Intermolecular interactions observed between the shortlisted penicillins and the M^{pro} protein

No	Name of ligand	Hydrogen Bonding Interactions	π- π stacking interactions	Hydrophobic interactions
1	Amoxicillin	His164, His41. Gly143, Thr26	His41	His41, Cys44, Met49, Cys145, His164, Met165
2	Ampicillin	His164, His41, Thr26	His41	His41, Cys44, Met49, Cys145, His164, Met165
3	Azidocillin	Glu166, His41, Gly143, Thr26	His41	His41, Cys44, Met49, Cys145, His164, Met165
4	Azlocillin	Glu166, Gln189, His41, Gly143, Thr26	His41	His41, Cys44, Met49, Cys145, His164, Met165
5	Benzylpenicillin	His41, Gly143, Thr26	His41	His41, Cys44, Met49, Cys145, His164, Met165
6	Carbenicillin	Glu166, His41, Gly143, Thr26	His41	His41, Cys44, Met49, Cys145, His164, Met165
7	Dicloxacillin	His41, Gly143, Thr26	His41	His41, Cys44, Met49, Cys145, His164, Met165
8	Phenoxymethylpenicillin	His41, Gly143, Thr26	His41	His41, Cys44, Met49, Cys145, His164, Met165
9	Piperacillin	His41, Gly143, Thr26	His41	His41, Cys44, Met49, Cys145, His164, Met165

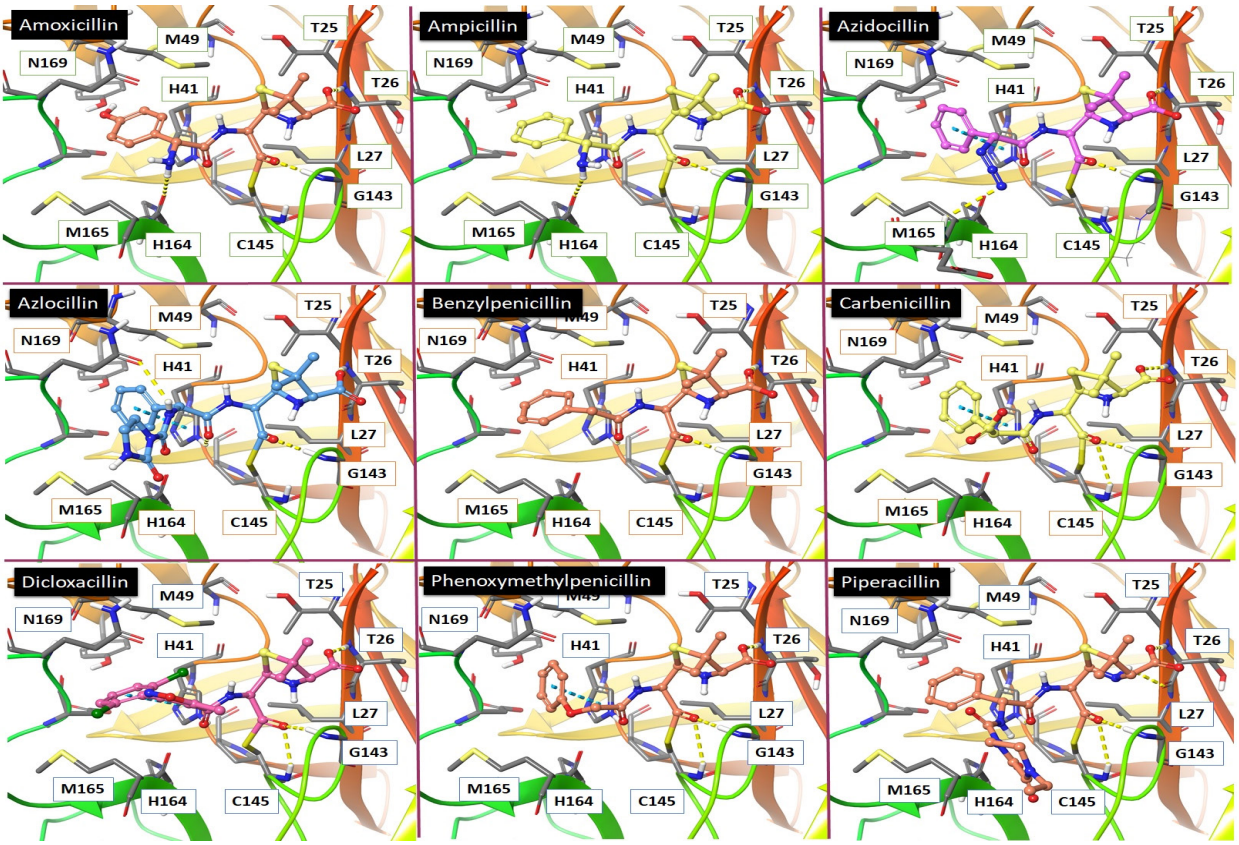

Figure 3. Covalent docking pose depicting the contact residues for Amoxicillin, Ampicillin, Azidocillin, Azlocillin, Benzylpenicillin, Carbenicillin, Dicloxacillin, Phenoxymethyl-penicillin and Piperacillin. The yellow colour dotted line represents the H-bond, cyan colour dotted line represents the π-π staking interaction.

(Figure 3).

The amine group formed H-bond interaction with residue His164, the amide carbonyl group formed H-bond with His41, the carbonyl group of opened β-lactam ring formed H-bond with residue Gly143, the carboxylate group formed H-bond with residue Thr26; the phenyl group formed the π-π staking interaction with His41; the residues His41, Cys44, Met49, Cys145, His164, Met165 formed hydrophobic interactions. The covalent docked pose of the ampicillin showed amalgam of polar and non-polar interactions. The amine group formed H-bond interaction with residue His164, the amide carbonyl group formed H-bond with His41, the carbonyl group of opened β-lactam ring formed H-bond with residue Gly143, the carboxylate group formed H-bond with residue Thr26; the phenyl group formed the π-π staking interaction with His41; the residues His41, Cys44, Met49, Cys145, His164, Met165 formed hydrophobic interactions.

The covalent docked pose of the Azidocillin displayed a combination of polar and non-polar interactions. The azide group formed H-bond interaction with residue Glu166, the amide carbonyl group formed H-bond with His41, the carbonyl group of opened β-lactam ring formed H-bond with residue Gly143, the carboxylate group formed H-bond with residue Thr26; the phenyl group formed the π-π staking interaction with His41; the residues His41, Cys44, Met49, Cys145, His164, Met165 formed hydrophobic interactions.

The covalent docked pose of the azlocillin exhibited a combination of polar and non-polar interactions. The nitrogen atom and the carbonyl group in the second position and the carbonyl group attached to the nitrogen of the imidazolidine-2-one formed H-bond with Glu166, the amine group formed H-bond interaction with residue Gln189, the amide carbonyl group formed H-bond with His41, the carbonyl group of opened β-lactam ring formed H-bond with residue Gly143, the carboxylate group formed H-bond with residue Thr26; the phenyl group formed the π-π staking interaction with His41; the residues His41, Cys44, Met49, Cys145, His164, Met165 formed hydrophobic interactions.

The covalent docked pose of the benzylpenicillin exhibited multiple polar and non-polar interactions with M^{pro} protein. The amide carbonyl group formed H-bond with His41, the carbonyl group of opened β-lactam ring formed H-bond with residue Gly143, the carboxylate group formed H-bond with residue Thr26; the phenyl group formed the π-π staking interaction with His41; the residues His41, Cys44, Met49, Cys145, His164, Met165 formed hydrophobic interactions.

The covalent docked pose of the carbenicillin exhibited a combination of polar and non-polar interactions with M^{pro} protein. The carboxylate group formed H-bond interaction with residue Glu166, the amide carbonyl group formed H-bond with His41, the carbonyl group of opened β-lactam ring formed H-bond with residue Gly143, the carboxylate group formed H-bond with residue Thr26; the phenyl group formed the π-π staking interaction with His41; the residues His41, Cys44, Met49, Cys145, His164, Met165 formed hydrophobic interactions.

The covalent docked pose of the Dicloxacillin exhibited multiple interactions with M^{pro} protein. The amide carbonyl group formed H-bond with His41, the carbonyl group of opened β-lactam ring formed H-bond with residue Gly143, the carboxylate group formed H-bond with residue Thr26; the phenyl group formed the π-π staking interaction with His41; the residues His41, Cys44, Met49, Cys145, His164, Met165 formed hydrophobic interactions.

The covalent docked pose of the Phenoxymethylpenicillin exhibited multiple interactions with M^{pro} protein. The amide carbonyl group formed H-bond with His41, the carbonyl group of opened β-lactam ring formed H-bond with residue Gly143, the carboxylate group formed H-bond with residue Thr26; the phenyl group formed the π-π staking interaction with His41; the residues His41, Cys44, Met49, Cys145, His164, Met165 formed hydrophobic interactions.

The covalent docked pose of the Piperacillin exhibited multiple interactions with M^{pro} protein. The amide carbonyl group formed H-bond with His41, the carbonyl group of opened β-lactam ring formed H-bond with residue Gly143, the carboxylate group formed H-bond with residue Thr26; the phenyl group formed the π-π staking interaction with His41; the residues His41, Cys44, Met49, Phe140, Leu141, Cys145, His163, His164, Met165 formed hydrophobic interactions.

Molecular Dynamics Simulations

The docking simulations does not consider the protein dynamics. So to check the stability of the covalent binding mode predicted for the β-lactams, MD simulation was carried out. All nine shortlisted penicillins were subjected to 100 ns MD simulation. The solvated system of the covalent docked complex with protein was checked for its binding stability based on the RMSD fluctuations during the simulation. The RMSD fluctuation measured individually for the protein and ligand structures in the trajectory of MD simulation, if it falls within 2.5 Å, then the complex considered to be stable. During the simulation, further, the persistence of the intermolecular interactions between the ligand and M^{pro} protein was also monitored. Figure 4 shows the RMSD plot for the ligand and protein during the MD simulation.

The analysis RMSD plot for the structures saved in the trajectory generated during the MD simulation exhibited stable binding for the benzylpenicillin and phenoxymethylpenicillin with M^{pro} protein where the RMSD fluctuations for the ligand and protein remained within 2.0 Å. The Ampicillin and Azlocillin, and Piperacillin exhibited moderate binding stability and rest of penicillins exhibited RMSD fluctuation higher than 3.0. Figure 4 lists the RMSD fluctuation and interaction consistency observed during the MD simulation for the nine shortlisted penicillins.

The M^{pro} covalent bound phenoxymethylpenicillin complex exhibited a steady binding mode during the MD simulation. The plot of the backbone of the protein structures enumerated during the MD simulation aligned to the initial structure for the RMSD analysis. After the initial fluctuation due to the equilibration, the RMSD for the protein structures remained between 1.2 Å to 2.5 Å till the end of the simulation (Figure 4). The fluctuations for the protein remained in between 1.3 Å indicated a stable protein structure. Similarly, the benzylpenicillin after the initial equilibration phase, the RMSD remained between 2.4 Å to 4.8 Å till the end of the simulation. The fluctuations remained in between 2.4 Å, indicating a stable ligand in the protein complex. Figure 5 depicts the ligand-protein contacts, and the protein-ligand contacts recorded during the MD simulation. The residues Asn142 and Cys145 exhibited an H-bond interaction with the ligand. The His41, Met49, Cys145 and Met165 exhibited hydrophobic interactions during the MD simulation. The Glu166 exhibited a water-mediated bridged interaction between ligand and protein. The majority of the interactions observed between the protein and ligand

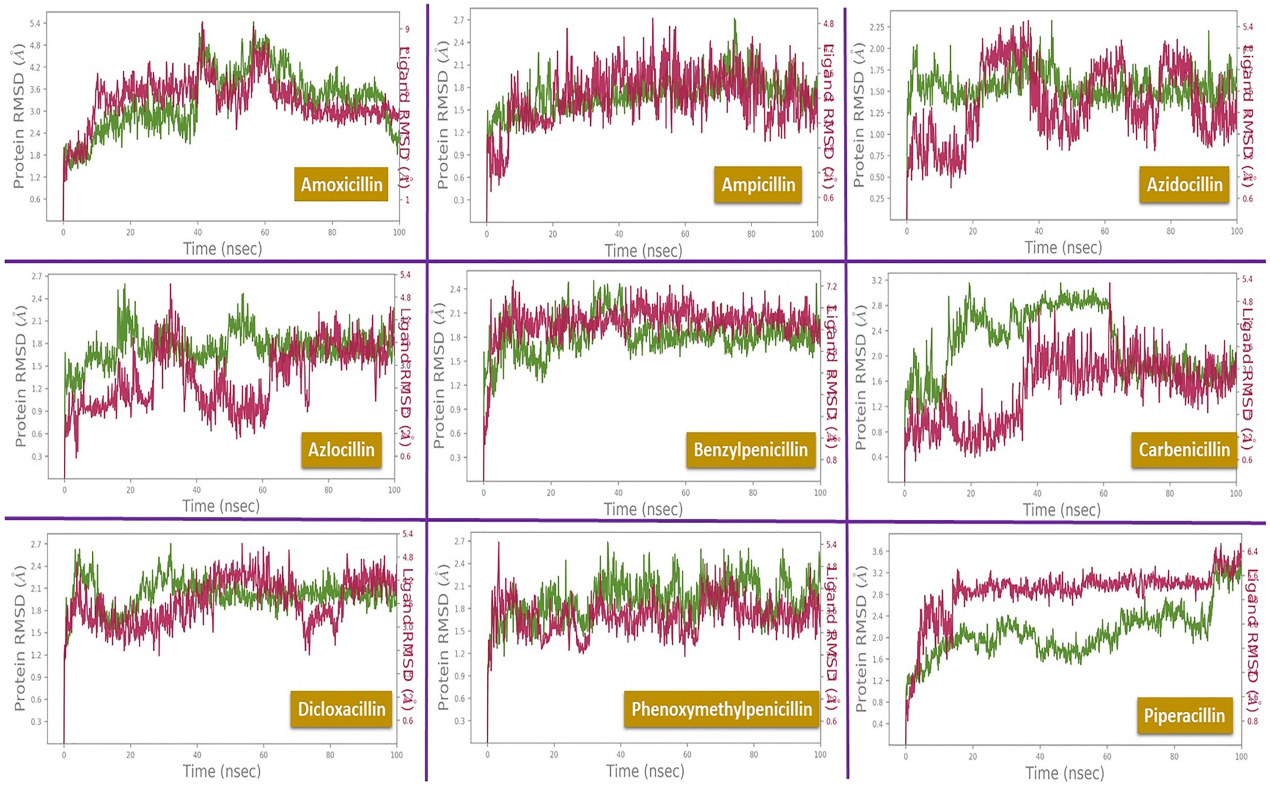

Figure 4. The Root Mean Square Deviations (RMSD) plots between the original structure and the structure enumerated during MD simulation. The protein backbone fluctuations are shown in green colour; ligand fluctuations are shown in red colour

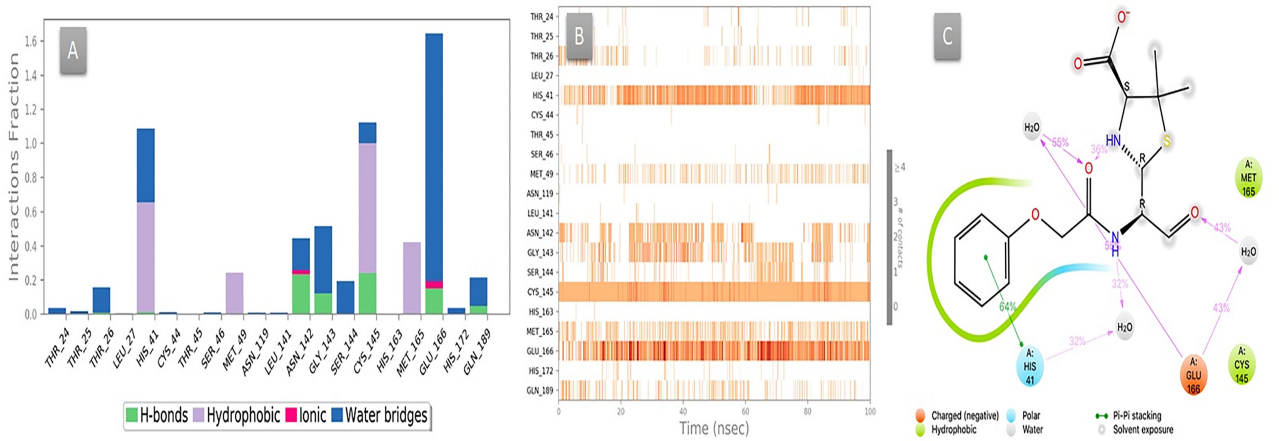

Figure 5. Interaction diagram of the Phenoxymethylpenicillin with M^{pro} protein observed during the molecular dynamics simulation. A: Protein-ligand interaction; B: Residues interact with the ligand in each trajectory frame. The residues making more than one contact are shown in darker colour shade; C: Schematic diagram of ligand interaction with the amino acid residues of protein during MD simulation. Interactions that occur more than 30% of the simulation time are shown.

during the docking were consistently retained during the MD simulation. The M^{pro} covalent bound Carbenicillin complex for the initial phase of the simulation exhibited higher fluctuations due to the equilibration. For the initial 60 ns of the simulation, the protein backbone exhibited higher RMSD fluctuation. The latter 40 ns the protein backbone fluctuations remained within the range of 1.0 Å, indicating stabilization of the protein structure. Similarly, the ligand showed a higher fluctuation for the initial 40 ns of the simulation. The ligand RMSD fluctuations remained within the range of 2.3 Å for the remaining 60 ns of the simulation indicated a stable ligand-protein complex. Figure 6 depicts the ligand-protein contacts, and the protein-ligand contacts recorded during the MD simulation. The residues Gln189, His41 and Cys145, exhibited H-bond interactions with the ligand. The His41, Cys145 and Met165 showed hydrophobic interactions during the MD simulation. The Glu166 exhibited a water-mediated bridged interaction between ligand and protein. The larger majority of the interactions observed between the M^{pro} and carbenicillin during the docking were retained during the MD simulation indicating stable binding mode prediction during the docking.

The M^{pro} covalent bound benzylpenicillin complex exhibited a consistent binding mode during the MD simulation. The plot of the backbone of the protein structures enumerated during the MD simulation aligned to the initial structure for the RMSD analysis. After the initial fluctuation due to the equilibration, the RMSD for the protein remained in between 1.2 Å indicated a stable protein structure. Similarly, the benzylpenicillin after the initial equilibration phase, the RMSD fluctuations remained in between 2.3 Å, indicating a stable ligand in the protein complex. During the initial phase of MD simulation, the benzyl moiety got flipped, but latter throughout the simulation, it remained consistent. The residues Ser144, Gly143, Asn142 and Cys145 exhibited consistent H-bond interactions, and the Cys145 exhibited hydrophobic interactions during the MD simulation. The Ampicillin exhibited a fluctuation of about 3.0 Å during the simulation, whereas the protein fluctuations were within 1.5 Å. The residues Glu166 exhibited an H-bond interaction and the His41, Cys145 and Met165 exhibited hydrophobic interactions between the ampicillin and M^{pro} during the MD simulation. The Azidocillin exhibited a fluctuation of about 3.5 Å during the simulation, whereas the protein fluctuations were within 1.0 Å. The residues Cys145 exhibited an H- bond interaction, the Glu166, Asn142 and Gly143 exhibited a water-mediated bridged interaction and the His41 and Met165 exhibited hydrophobic interactions between the azidocillin and M^{pro} during the MD simulation. The other penicillins during the MD simulation exhibited higher structural fluctuations for the ligand considered during the simulation indicated lac of binding stability between the protein and ligand.

In summary, the docking of the penicillins to M^{pro} resulted in the binding model where the β-lactam ring. Further, the FDA approved β-lactam containing molecules were covalently binding to M^{pro}. The nine molecules Amoxicillin, Ampicillin, Azidocillin, Azlocillin, Benzylpenicillin, Carbenicillin, Dicloxacillin, Phenoxymethylpenicillin and Piperacillin, exhibited the same binding orientation and interaction pattern. The molecular dynamics simulation revealed that Phenoxymethylpenicillin and Carbenicillin complex has good binding stability compared to other penicillins. Testing for in vitro M^{pro} protease inhibitory activity, and antiviral activity, could confirm if penicillins or β-lactams could be repurposed or repositioned for anti-COVID-2 treatment. Generally, the chances of antimicrobial-resistance are high when antibiotics are given with antiviral agents. But in COVID-19, the antibiotic Azithromycin was used along with hydroxychloroquine. The penicillins are milder and less potent compared to Azithromycin, and hence we suggest that the penicillin such as Phenoxymethylpenicillin and Carbenicillin can be tried along with hydroxyquinoline for COVID-19.

Conclusion

Currently, no pharmacotherapy is available against CoV disease, which makes it curtail for the researchers to

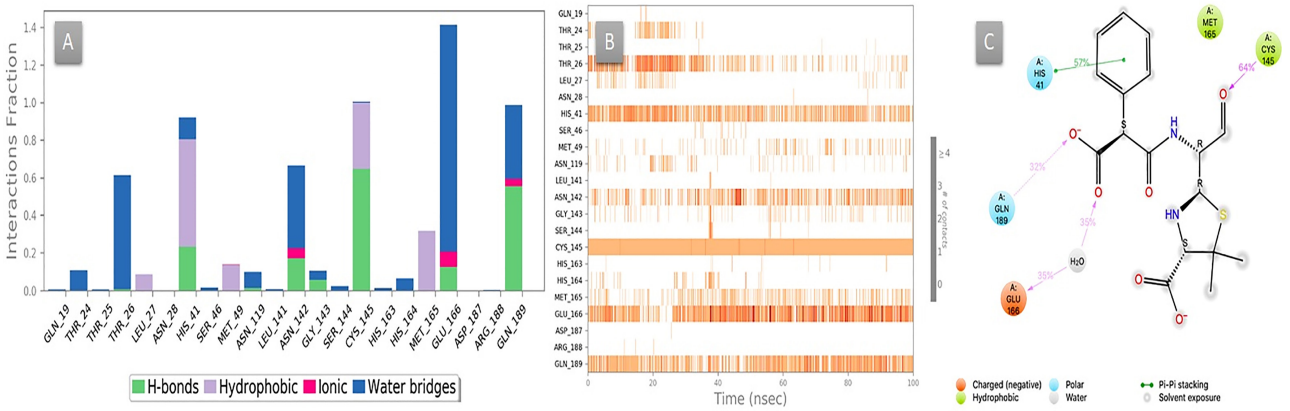

Figure 6. Interaction diagram of the Carbenicillin with M^{pro} protein observed during the molecular dynamics simulation
A: The protein-ligand interaction diagram. B: The residues that interact with the ligand in each trajectory frame. The residues making more than one contact are shown in darker colour shade. C: Schematic diagram of ligand interaction with the amino acid residues of protein during MD simulation. Interactions that occur more than 30% of the simulation time are shown

utilise new techniques to fast-track the drug identification process for the same. The genetic material in CoVs is highly susceptible to mutations, and there were incidences of altered virulence and human pandemic outbreaks. In our study, the computer-aided drug design technique was utilised to identify drugs which can be repurposed for SARS-CoV-2 protein M^{pro}. Schrodinger software was utilised to conduct the study. The study showed that penicillin compounds consistent binding to M^{pro}. Further, we found Phenoxymethylpenicillin and Carbenicillin have high potential to act as anti-CoV agent. Thus, this study results can be utilised further for testing in vitro and in vivo assays.

Acknowledgements

Authors are thankful to Manipal Academy of Higher Education, Manipal for TMA Pai fellowship for PhD to Krishnaprasad B and Akhil Suresh. Authors are also grateful to ICMR, New Delhi, as Swastika Maity is working under ICMR-SRF (45/33/2019/PHA/BMS). Authors are thankful to Department of Pharmaceutics, Manipal College of Pharmaceutical Sciences facilitating the computer simulations. Schrodinger's Software and Computers were procured under the grant from DST-SERB, New Delhi to Usha YN ([EMR/2016/007006).

Conflict of Interest

The authors declare that they do not have any conflict of interest in publishing these data.

References

1. Guo YR, Cao QD, Hong ZS, Tan YY, Chen SD, Jin HJ, et al. The origin, transmission and clinical therapies on coronavirus disease 2019 (COVID-19) outbreak-A n update on the status. Mil Med Res. 2020;7:11. doi:10.1186/s40779-020-00240-0
2. Shereen MA, Khan S, Kazmi A, Bashir N, Siddique R. COVID-19 infection: Origin, transmission, and characteristics of human coronaviruses. J Adv Res. 2020;24:91-8. doi:10.1016/j.jare.2020.03.005
3. Zheng J. SARS-CoV-2: an Emerging Coronavirus that Causes a Global Threat. Int J Biol Sci. 2020;16(10):1678-85. doi:10.7150/ijbs.45053
4. Zhu N, Zhang D, Wang W, Li X, Yang B, Song J, et al. A novel coronavirus from patients with pneumonia in China, 2019. N Engl J Med. 2020;382(8):727-33. doi:10.1056/NEJMoa2001017
5. Gorbalenya AE, Baker SC, Baric RS, de Groot RJ, Drosten C, Gulyaeva AA, et al. The species Severe acute respiratory syndrome-related coronavirus: classifying 2019-nCoV and naming it SARS-CoV-2. Nat Microbiol. 2020;5(4):536-44. doi:10.1038/s41564-020-0695-z
6. Ye ZW, Yuan S, Yuen KS, Fung SY, Chan CP, Jin DY. Zoonotic origins of human coronaviruses. Int J Biol Sci. 2020;16(10):1686-97. doi:10.7150/ijbs.45472
7. Mousavizadeh L, Ghasemi S. Genotype and phenotype of COVID-19: Their roles in pathogenesis. J Microbiol Immunol Infect. 2020. doi:10.1016/j.jmii.2020.03.022
8. Zhang J, Litvinova M, Wang W, Wang Y, Deng X, Chen X, et al. Evolving epidemiology and transmission dynamics of coronavirus disease 2019 outside Hubei province, China: a descriptive and modelling study. Lancet Infect Dis. 2020;20(7):793-802. doi:10.1016/S1473-3099(20)30230-9
9. Liu J, Liao X, Qian S, Yuan J, Wang F, Liu Y, et al. Community transmission of severe acute respiratory syndrome coronavirus 2, Shenzhen, China, 2020. Emerg Infect Dis. 2020;26(6):1320-23. doi:10.3201/eid2606.200239
10. Ong SWX, Tan YK, Chia PY, Lee TH, Ng OT, Wong MSY, et al. Air, surface environmental, and personal protective equipment contamination by severe acute respiratory syndrome coronavirus 2 (SARS-CoV-2) from a symptomatic patient. JAMA. 2020;323(16):1610-12. doi:10.1001/jama.2020.3227
11. Wu Y, Guo C, Tang L, Hong Z, Zhou J, Dong X, et al. Prolonged presence of SARS-CoV-2 viral RNA in faecal samples. Lancet Gastroenterol Hepatol. 2020;5(5):434-5. doi:10.1016/S2468-1253(20)30083-2
12. Kannan S, Shaik Syed Ali P, Sheeza A, Hemalatha K. COVID-19 (Novel Coronavirus 2019) - recent trends. Eur Rev Med Pharmacol Sci. 2020;24(4):2006-11. doi:10.26355/eurrev_202002_20378
13. Zhang H, Penninger JM, Li Y, Zhong N, Slutsky AS. Angiotensin-converting enzyme 2 (ACE2) as a SARS-CoV-2 receptor: molecular mechanisms and potential therapeutic target. Intensive Care Med. 2020;46(4):586-90. doi:10.1007/s00134-020-05985-9
14. Gao Y, Yan L, Huang Y, Liu F, Zhao Y, Cao L, et al. Structure of the RNA-dependent RNA polymerase from COVID-19 virus. Science. 2020;368(6492):779-82. doi:10.1126/science.abb7498
15. Kandeel M, Al-Nazawi M. Virtual screening and repurposing of FDA approved drugs against COVID-19 main protease. Life Sci. 2020;251:117627. doi:10.1016/j.lfs.2020.117627
16. Chan KW, Wong VT, Tang SCW. COVID-19: An update on the epidemiological, clinical, preventive and therapeutic evidence and guidelines of integrative chinese-western medicine for the management of 2019 novel coronavirus disease. Am J Chin Med. 2020;48(3):737-62. doi:10.1142/S0192415X20500378
17. Ton AT, Gentile F, Hsing M, Ban F, Cherkasov A. Rapid identification of potential inhibitors of SARS-CoV-2 main protease by deep docking of 1.3 billion compounds. Mol Inform. 2020;39(8):e2000028. doi:10.1002/minf.202000028
18. Prajapat M, Sarma P, Shekhar N, Avti P, Sinha S, Kaur H, et al. Drug targets for corona virus: A systematic review. Indian J Pharmacol. 2020;52(1):56-65. doi:10.4103/ijp.IJP_115_20
19. McGonagle D, Sharif K, O'Regan A, Bridgewood C. The Role of cytokines including interleukin-6 in COVID-19 induced pneumonia and macrophage

activation syndrome-like disease. Autoimmun Rev. 2020;19(6):102537. doi:10.1016/j.autrev.2020.102537
20. Giwa A, Desai A. Novel coronavirus COVID-19: an overview for emergency clinicians. Emerg Med Pract. 2020;22(2):1-21.
21. Jin Y, Yang H, Ji W, Wu W, Chen S, Zhang W, et al. Virology, epidemiology, pathogenesis, and control of covid-19. Viruses. 2020;12(4):372. doi:10.3390/v12040372
22. Mehta P, McAuley DF, Brown M, Sanchez E, Tattersall RS, Manson JJ, HLH Across Speciality Collaboration UK. COVID-19: consider cytokine storm syndromes and immunosuppression. Lancet. 2020;395(10229):1033-4. doi:10.1016/S0140-6736(20)30628-0.
23. Devaux CA, Rolain J-M, Colson P, Raoult D. New insights on the antiviral effects of chloroquine against coronavirus: what to expect for COVID-19? Int J Antimicrob Agents. 2020;55(5):105938. doi:10.1016/j.ijantimicag.2020.105938.
24. Liu C, Zhou Q, Li Y, Garner L V, Watkins SP, Carter LJ, et al. Research and development on therapeutic agents and vaccines for COVID-19 and related human coronavirus diseases. ACS Cent Sci. 2020;6(3):315-31. doi:10.1021/acscentsci.0c00272.
25. Kupferschmidt K, Cohen J. Race to find COVID-19 treatments accelerates. Science. 2020;367(6485):1412-13. doi:10.1126/science.367.6485.1412
26. Yao TT, Qian JD, Zhu WY, Wang Y, Wang GQ. A systematic review of lopinavir therapy for SARS coronavirus and MERS coronavirus—A possible reference for coronavirus disease-19 treatment option. J Med Virol. 2020;92(6):556-63. doi:10.1002/jmv.25729
27. Elfiky AA. Ribavirin, Remdesivir, Sofosbuvir, Galidesivir, and Tenofovir against SARS-CoV-2 RNA dependent RNA polymerase (RdRp): A molecular docking study. Life Sci. 2020;117592. doi:10.1016/j.lfs.2020.117592
28. Zhang R, Wang X, Ni L, Di X, Ma B, Niu S, et al. In silico studies on therapeutic agents for COVID-19: Drug repurposing approach. Life Sci. 2020;252:117652. doi:10.1016/j.lfs.2020.117592.
29. Elfiky AA. Anti-HCV, nucleotide inhibitors, repurposing against COVID-19. Life Sci. 2020;248:117477. doi:10.1016/j.lfs.2020.117477.
30. Lai CC, Shih TP, Ko WC, Tang HJ, Hsueh PR. Severe acute respiratory syndrome coronavirus 2 (SARS-CoV-2) and coronavirus disease-2019 (COVID-19): The epidemic and the challenges. Int J Antimicrob Agents. 2020;55(3):105924. doi:10.1016/j.ijantimicag.2020.105924
31. Cao B, Wang Y, Wen D, Liu W, Wang J, Fan G, et al. A trial of lopinavir–ritonavir in adults hospitalized with severe Covid-19. N Engl J Med. 2020;382(19):1787-99. doi:10.1056/nejmoa2001282.
32. Manica Negahdaripour. The battle against COVID-19: where do we stand now? Iran J Med Sc. 2020;45(2):81-2. doi:10.3390/v12020244.
33. Cai Q, Yang M, Liu D, Chen J, Shu D, Xia J, et al. Experimental treatment with favipiravir for COVID-19: an open-label control study. Engineering. 2020. doi:10.1016/j.eng.2020.03.007
34. Jin Z, Du X, Xu Y, Deng Y, Liu M, Zhao Y, et al. Structure of M^{pro} from COVID-19 virus and discovery of its inhibitors. BioRxiv. 2020. doi:10.1101/2020.02.26.964882
35. Li J, Ma X-B, Shen J, Zhang Z-F. Screening of active components from Chinese materia medica against SARS-CoV-2 based on literature mining and molecular docking. Chinese Trad Herb Drugs. 2020;51(4):845-50. doi:10.7501/j.issn.0253-2670.2020.04.003
36. Chen I-J, Foloppe N. Drug-like bioactive structures and conformational coverage with the ligprep/confgen suite: Comparison to programs MOE and catalyst. J Chem Inf Model. 2010;50(5):822-39. doi:10.1021/ci100026x
37. 37. Roos K, Wu C, Damm W, Reboul M, Stevenson JM, Lu C, et al. OPLS3e: Extending force field coverage for drug-like small molecules. J Chem Theory Comput. 2019;15(3):1863-74. doi:10.1021/acs.jctc.8b01026
38. Madhavi Sastry G, Adzhigirey M, Day T, Annabhimoju R, Sherman W. Protein and ligand preparation: Parameters, protocols, and influence on virtual screening enrichments. J Comput Aided Mol Des. 2013;27(3):221-34. doi:10.1007/s10822-013-9644-8
39. Rostkowski M, Olsson MH, Søndergaard CR, Jensen JH. Graphical analysis of pH-dependent properties of proteins predicted using PROPKA. BMC Struct Biol. 2011;11:6. doi:10.1186/1472-6807-11-6.
40. Olsson MHM, Søndergaard CR, Rostkowski M, Jensen JH. PROPKA3: Consistent treatment of internal and surface residues in empirical pKa predictions. J Chem Theory Comput. 2011;7(2):525-37. doi:10.1021/ct100578z
41. Halgren TA, Murphy RB, Friesner RA, Beard HS, Frye LL, Pollard WT, et al. Glide: a new approach for rapid, accurate docking and scoring. 2. Enrichment factors in database screening. J Med Chem. 2004;47(7):1750-9. doi:10.1021/jm030644s
42. Friesner RA, Banks JL, Murphy RB, Halgren TA, Klicic JJ, Mainz DT, et al. Glide: a new approach for rapid, accurate docking and scoring. 1. Method and assessment of docking accuracy. J Med Chem. 2004;47(7):1739-49. doi:10.1021/jm0306430
43. Toledo Warshaviak D, Golan G, Borrelli KW, Zhu K, Kalid O. Structure-based virtual screening approach for discovery of covalently bound ligands. J Chem Inf Model. 2014;54(7):1941-50. doi:10.1021/ci500175r
44. Zhu K, Borrelli KW, Greenwood JR, Day T, Abel R, Farid RS, et al. Docking covalent inhibitors: A parameter free approach to pose prediction and scoring. J Chem Inf Model. 2014;54(7):1932-40. doi:10.1021/ci500118s

45. Bowers KJ, Chow E, Xu H, Dror RO, Eastwood MP, Gregersen BA, et al. Scalable algorithms for molecular dynamics simulations on commodity clusters. Proc 2006 ACM/IEEE Conf Supercomput SC'06. 2006. doi:10.1145/1188455.1188544.
46. Kandeel M, Ibrahim A, Fayez M, Al-Nazawi M. From SARS and MERS CoVs to SARS-CoV-2: Moving toward more biased codon usage in viral structural and nonstructural genes. J Med Virol. 2020;92(6):660-6. doi:10.1002/jmv.25754
47. Wu C, Liu Y, Yang Y, Zhang P, Zhong W, Wang Y, et al. Analysis of therapeutic targets for SARS-CoV-2 and discovery of potential drugs by computational methods. Acta Pharm Sin B. 2020;10(5):766-88 doi:10.1016/j.apsb.2020.02.008
48. Yoakim C, Ogilvie WW, Cameron DR, Chabot C, Grand-Maître C, Guse I, et al. β-Lactam derivatives as inhibitors of human cytomegalovirus protease. J Med Chem. 1998;41:2882-91. doi:10.1177/095632029800900502
49. Veinberg G, Potorocina I, Vorona M. Recent trends in the design, synthesis and biological exploration of β -lactams. Curr Med Chem. 2014;21(4):393-416. doi: 10.2174/09298673113206660268